Supplemental Figure S1.

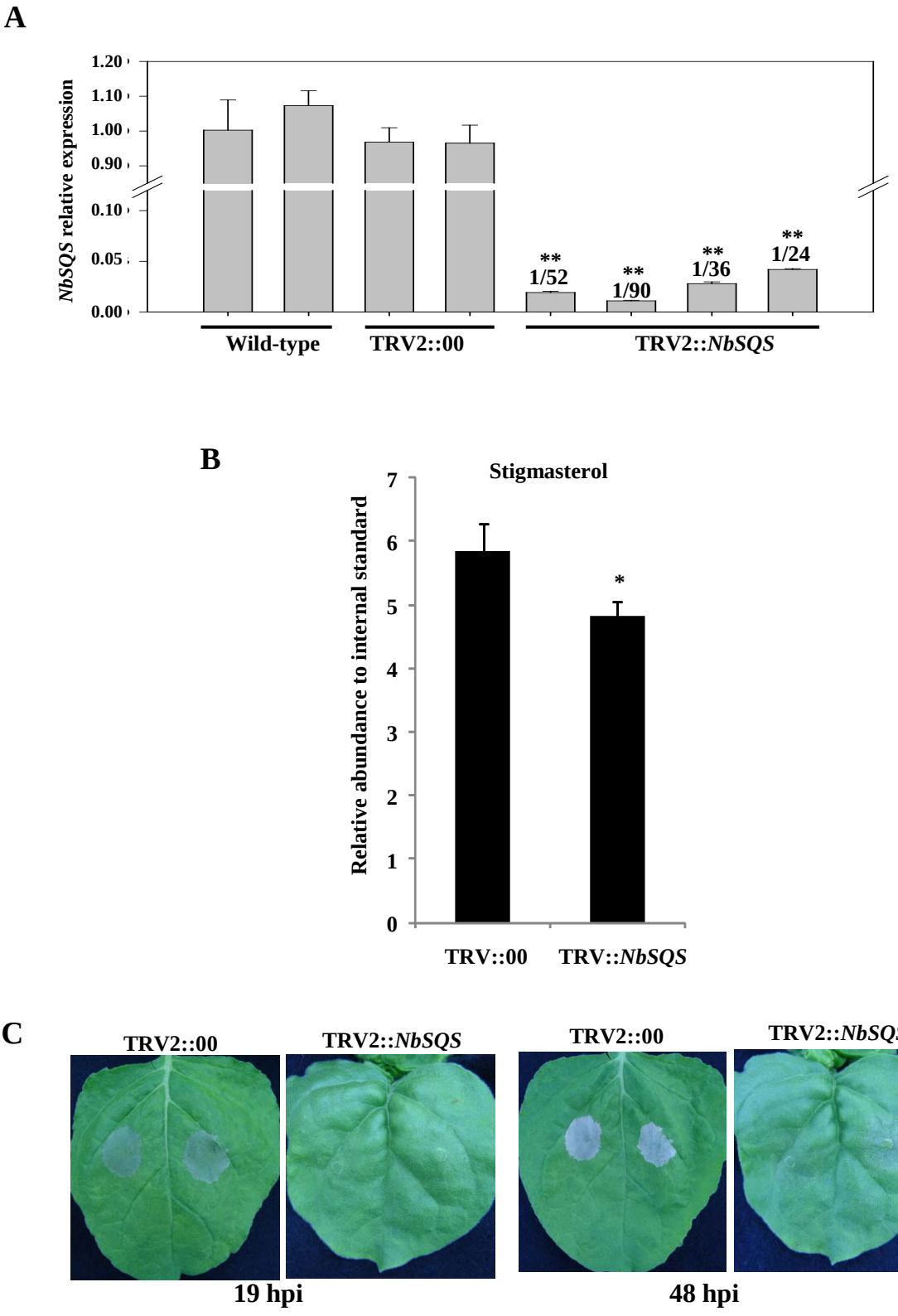

D

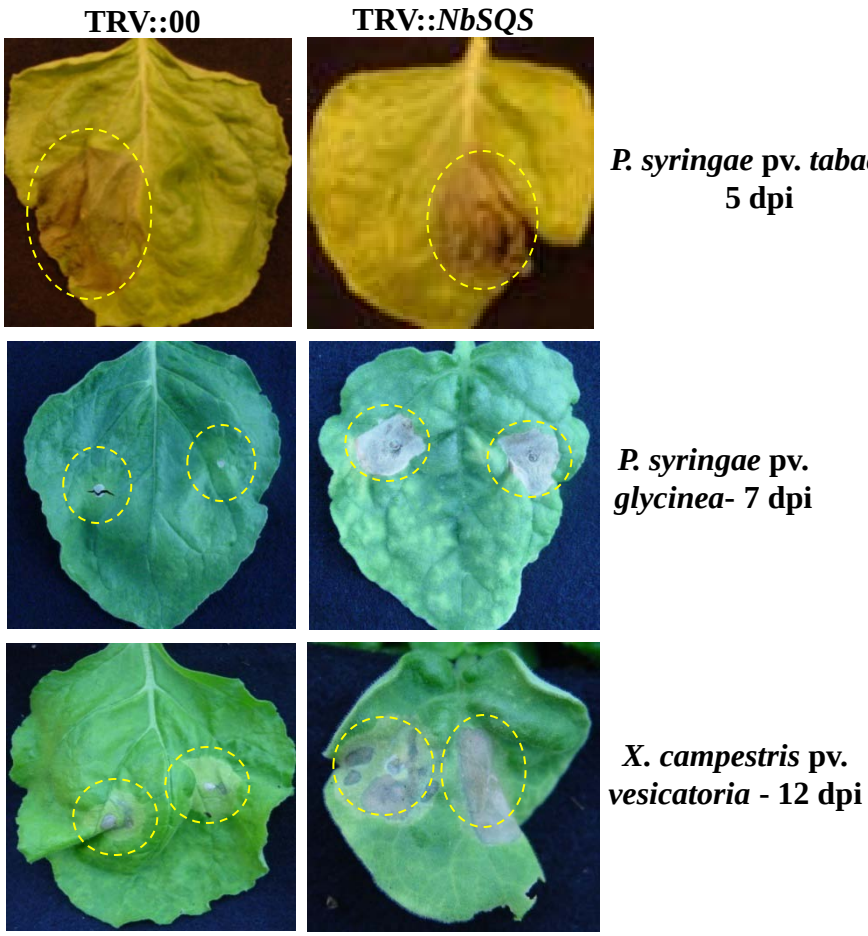

Supplemental Figure S1. Endogenous *NbSQS* gene transcript levels, sterol levels, occurrence of hypersensitive response (HR) and disease symptoms in *NbSQS*-gene-silenced plants

A, *N. benthamiana* plants were infiltrated with *A. tumefaciens* GV2260 carrying TRV1 and TRV2::*NbSQS*. After three weeks, relative expression of *NbSQS* in the *NbSQS*-silenced and control plants was determined by real-time PCR. Values above bars indicate the ratio of *NbSQS* transcript in TRV2::*NbSQS*- silenced plants to the wild-type. Asterisks indicate the significant difference from the wild-type ($P<0.001$). Data were pooled from two independent experiments representing four biological replicates.

B, Sterols were estimated from the gene-silenced upper leaves using the GC-MS-based protocol described in the Materials and Methods section. Relative abundance to the internal standard is presented here. Ions were identified by MET-IDEA software with corresponding I/Z values for stigmasterol. Changes were verified with a chromatogram developed using corresponding standards (AMDIS software, http://www.amdis.net/What_is_AMDIS/AMDIS_Advanced/amdis_advanced.html and MET-IDEA software, http://bioinfo.noble.org/download/?download_id=1). Data were pooled from two independent experiments representing five biological replicates.

C, Hypersensitive reactions of the silenced *N. benthamiana* plant to the nonhost pathogen *Pst* T1. Upper leaves of silenced *N. benthamiana* plants were challenged with *Pst* T1 at a concentration of 2×10^7 cfu/ml. Pictures of HR cell death symptoms were taken 19 hours and 48 hours after inoculation.

D, Disease symptoms of silenced *N. benthamiana* plants were assessed by spot inoculation of respective host and nonhost pathogens. Pictures were taken at the indicated time. Inoculated spots are circled.

Supplemental Figure S2.

A

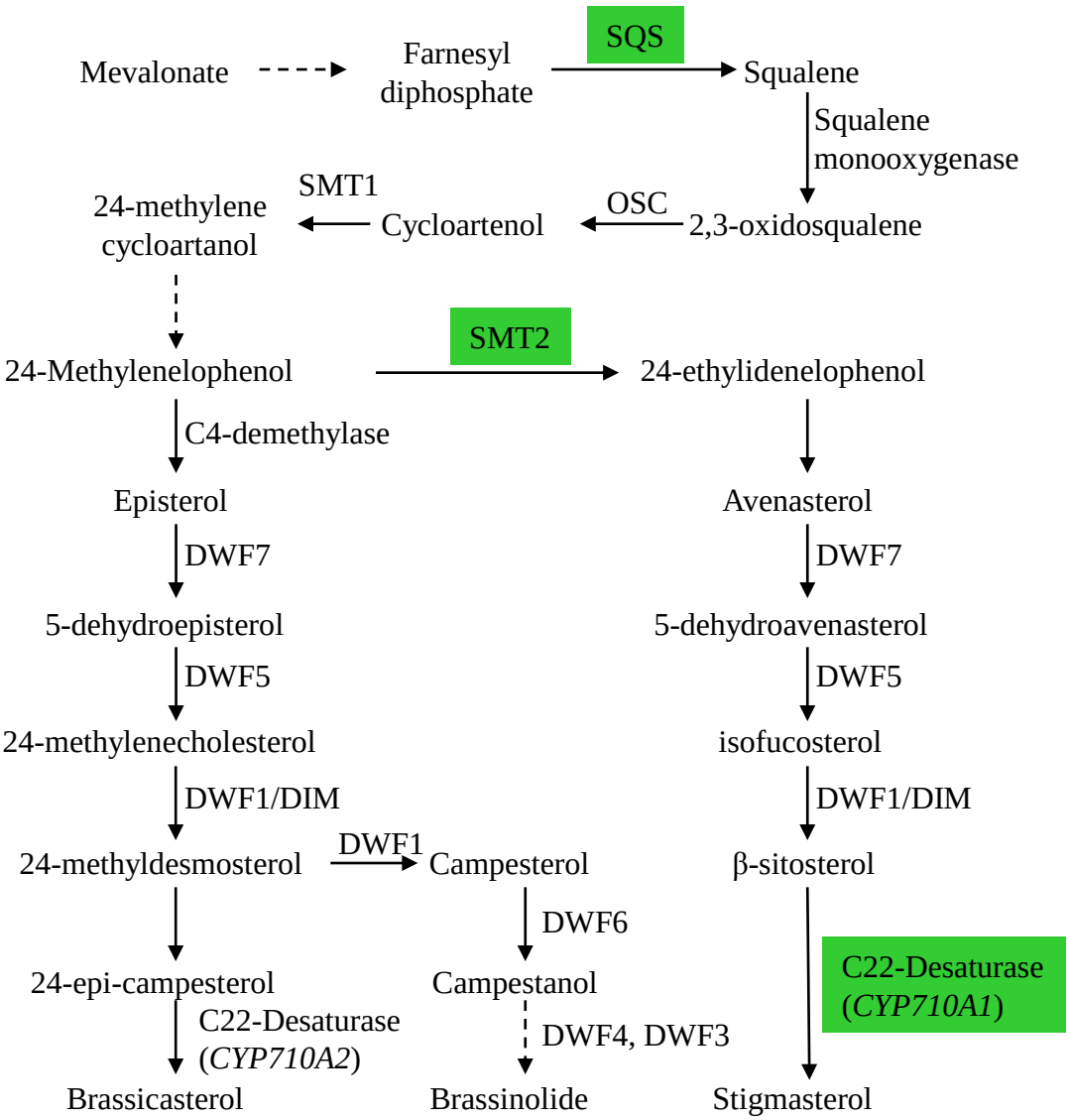

Modified from:
Schrick, K., Fujioka, S., Takatsuto, S., Stierhof, Y.D., Stransky, H., Yoshida, S., Jurgens, G. (2004). A link between sterol biosynthesis, the cell wall, and cellulose in Arabidopsis. The Plant Journal *38, 227-243.*

B

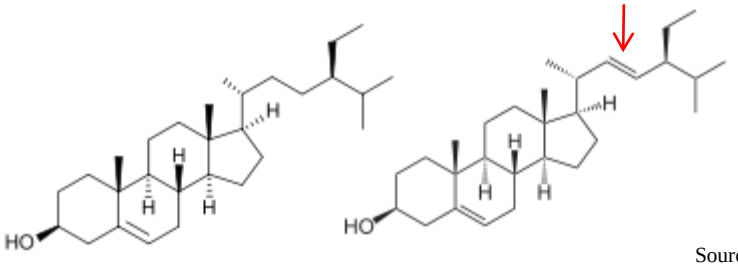

Source: http://en.wikipedia.org/

β-sitosterol **Stigmasterol**

C

TRV2::00 **TRV2::*NbSQS***

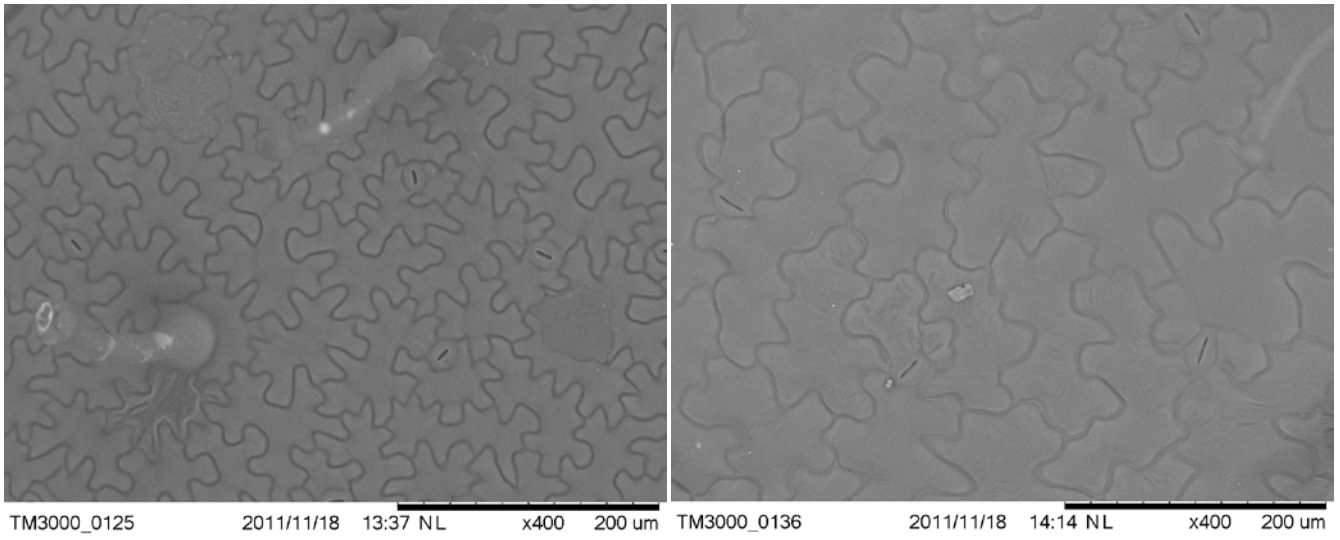

D **TRV2::00**

No stress (control) **Heat stress**

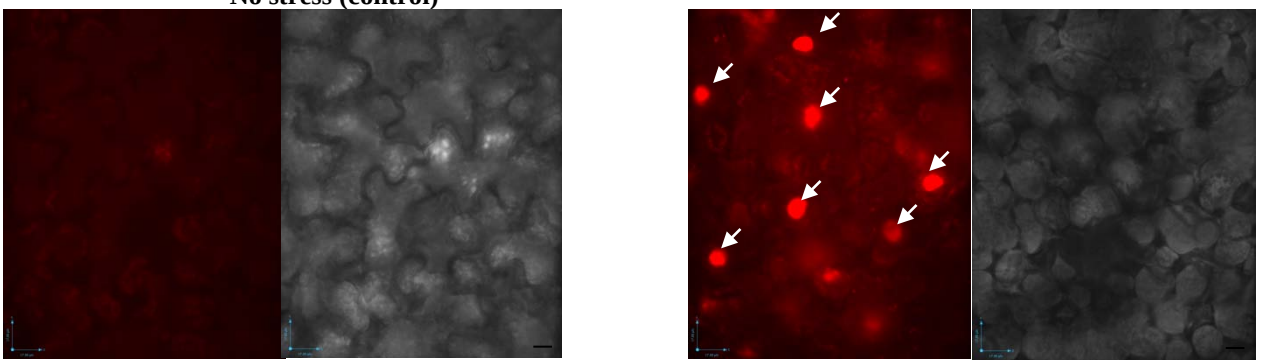

E **TRV2::*NbSQS***

No stress (control) **Heat stress**

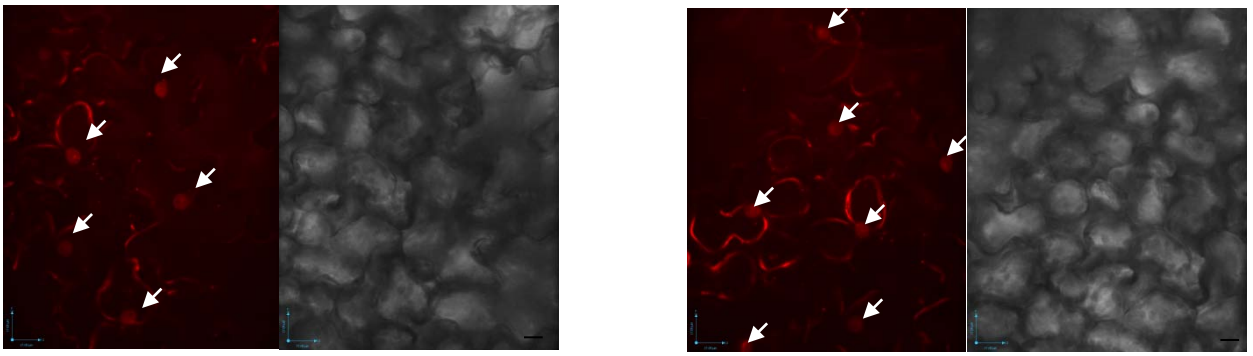

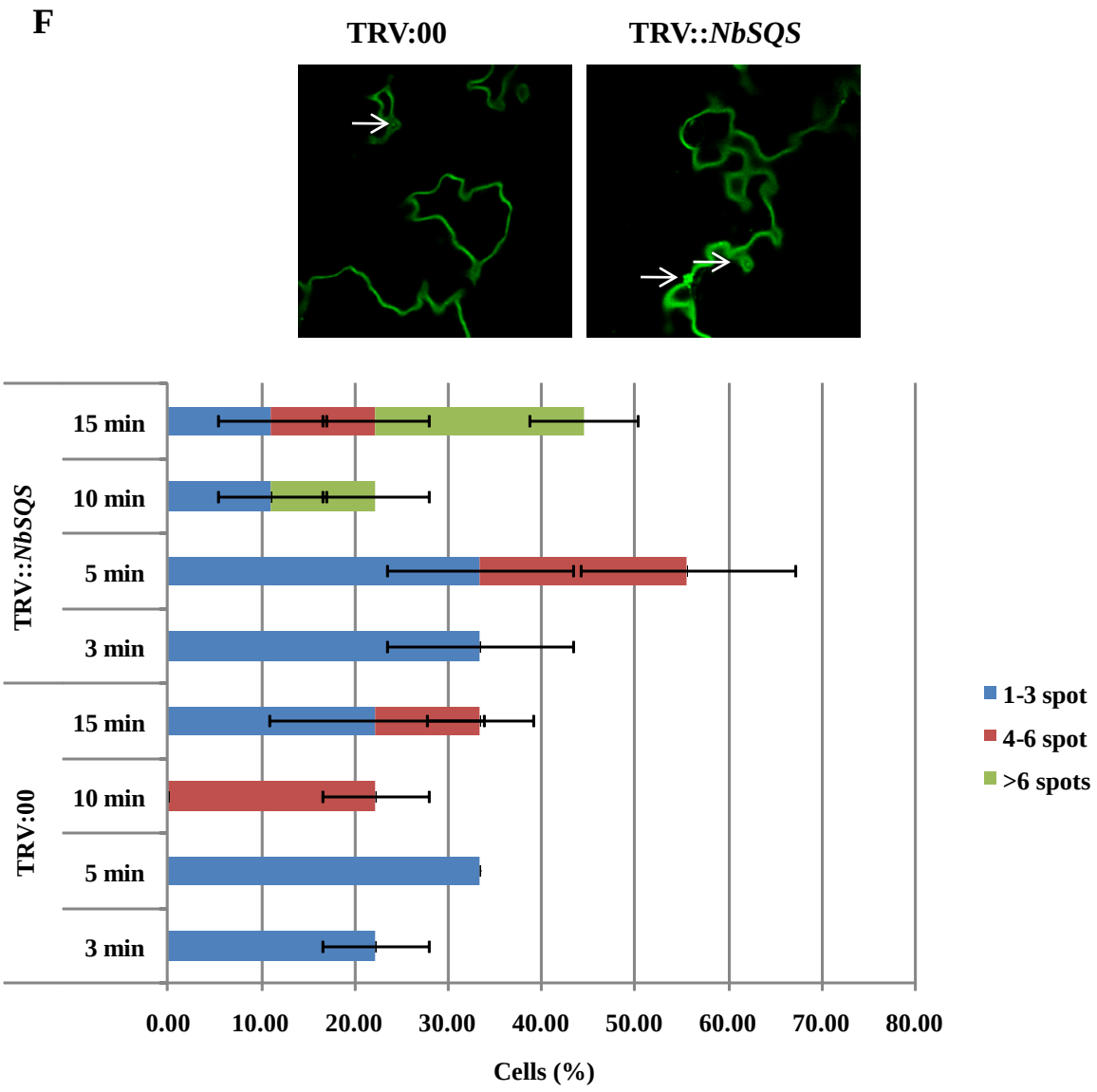

Supplemental Figure S2. Simplified biosynthetic pathway for plant sterols and structure of β-sitosterol and stigmasterol. A, Sterol biosynthetic pathway; B, Structure of β-sitosterol and stigmasterol.
C, To study the cell shape and size, leaf segments from TRV:00 and TRV::*NbSQS* plants were viewed under a scanning electron microscope (TM3000).
D, Assessing the penetration of propidium iodide dye in heat stressed leaf tissues. Leaf tissues were collected from TRV:00 plants and dipped in 70^{o}C water for 3 minutes. Both control and heat stressed tissues were incubated in propidium iodide solution. Sections were made from these leaf segments and observed for cells stained for their nuclei, and the number of cells showing nuclei staining were counted under confocal microscope (Perkin Elmer ultra view ERS spinning disk confocal).
F, Extent of FM1-43 dye internalization – visual qualitative assessment. Extent of the penetration of FM1-43 dyes into *NbSQS*-gene-silenced *N. benthamiana* plant cells. Leaf tissues were collected from TRV:00 and TRV::*NbSQS*-gene-silenced *N. benthamiana* plants and incubated in solution containing FM1-43 dye. The cytoplasmic contents stained with FM1-43 were observed under confocal microscope (Leica TCS SP2 AOBS confocal laser scanning microscope). At the indicated time intervals, a total of three cells showing internalization of dye were scored as three class intervals (as shown). Percentage of cells showing dye entry is plotted. Top panel shows a representative image at 3 min.

Supplemental Figure S3

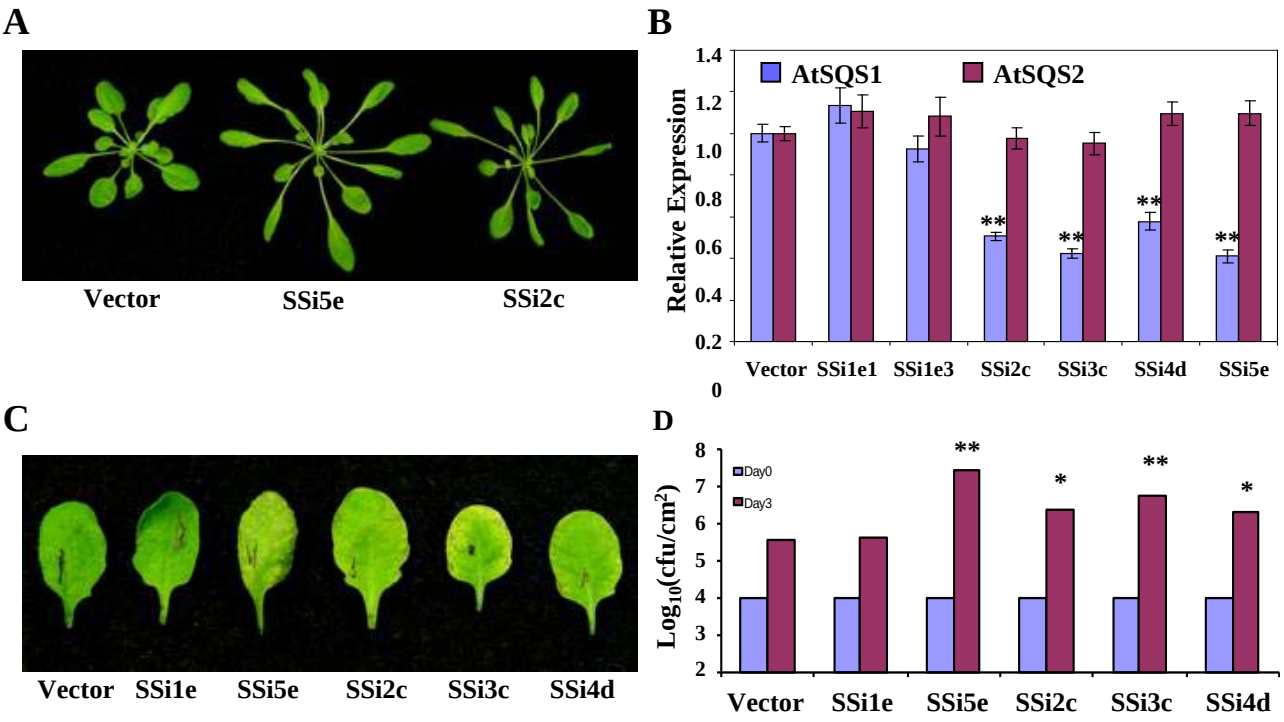

Supplemental Figure S3. Silencing of the *AtSQS1* gene and *smt2* mutation in Arabidopsis leads to disease susceptibility. A, Phenotype of Arabidopsis *AtSQS1* RNAi lines (SSi5e and SSi2c). Both vector control and RNAi lines were grown under control conditions, and 4-week-old plants were photographed. B, Relative expression of *AtSQS1* in different transgenic *AtSQS1* RNAi lines to vector control examined by qRT-PCR. C, Nonhost pathogen *P. syringae* pv. *tabaci* was infiltrated into 4-week-old Arabidopsis plant leaves at a concentration of ~1×10^6 cfu/ml. Photographs of disease symptoms were taken at 4 dpi. D, Bacterial growth was determined at 0 and 3 dpi. Asterisks indicate the significant difference from the wild-type (*P<0.05 and **P<0.001). Data were pooled from two independent experiments representing four biological replicates.

Supplemental Figure S4

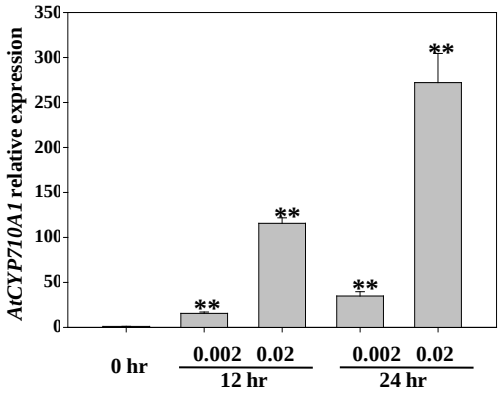

Supplemental Figure S4. Dosage-dependent expression of the *AtCYP710A1* gene upon nonhost pathogen inoculation. Arabidopsis Col-0 plants were vacuum-infiltrated with *P. syringae* pv. *tabaci* at concentrations of ~1×10^5 cfu/ml (OD_{600}=0.002) and ~1×10^6 cfu/ml (OD_{600}=0.02). The leaf tissues were collected at 12 and 24 hpi. The relative expression of *AtCYP710A1* to 0 hr time point at different time points before inoculation was determined by qRT-PCR. Asterisks indicate the significant difference from the wild-type (*P<0.05 and **P<0.001). Data were pooled from two independent experiments representing four biological replicates.

Supplemental Figure S5

A

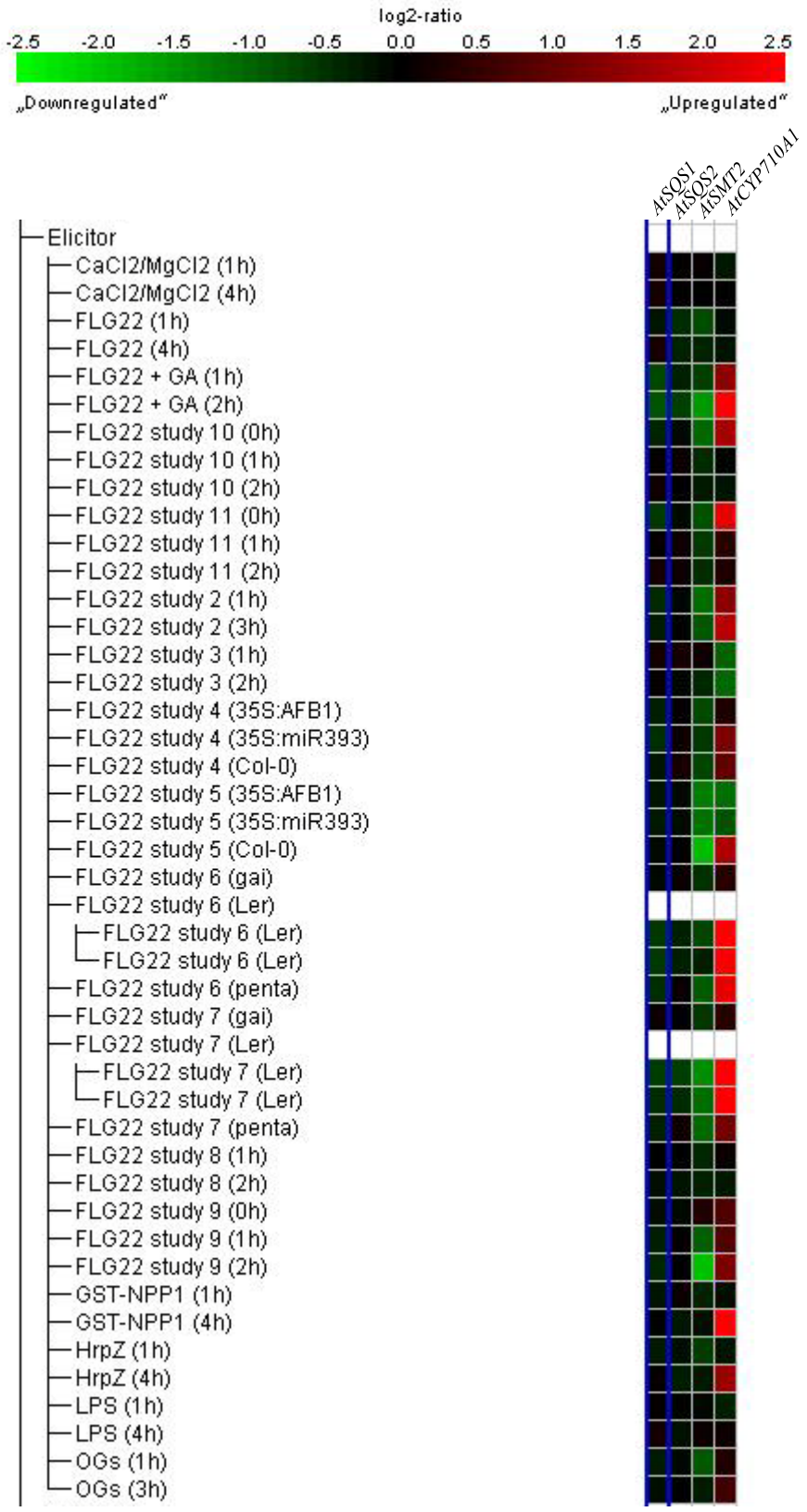

B

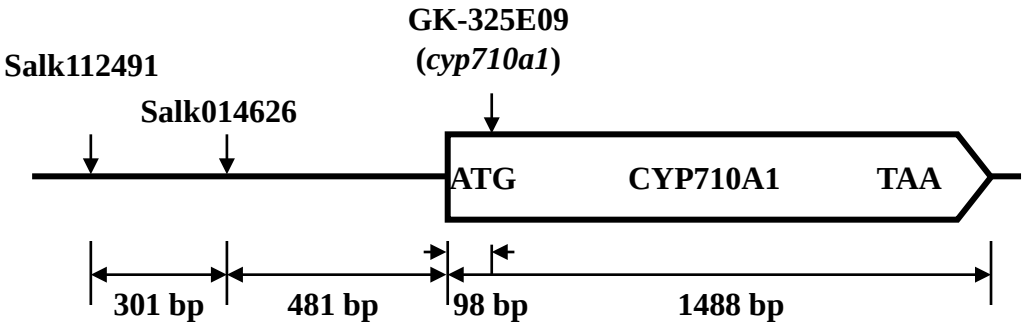

C

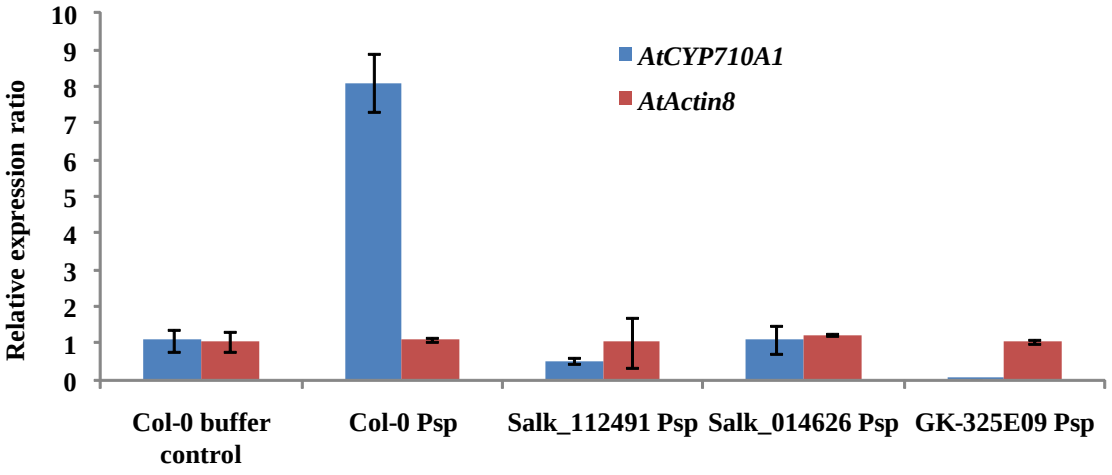

D

Wild type (Col 0) | *Atcyp710A1*-48 | *Atcyp710A1*-52

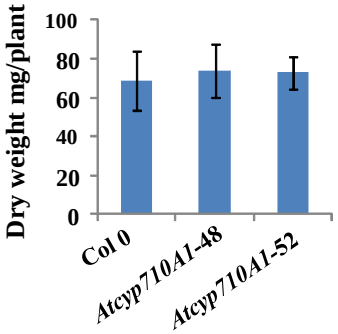

E

Wild type (Col 0) | ***Atcyp710A1*-48** | ***Atcyp710A1*-52**

Supplemental Figure S5. *AtCYP710A1* gene expression upon elicitor treatment and details of Arabidopsis *Atcyp710A1* mutants.

A, *AtCYP710A1* gene transcripts are induced by PAMP elicitors. We used the publicly available GENEVESTIGATOR database (https://www.genevestigator.com/gv/index.jsp) to know the transcript expression pattern of AtSQS1, AtSQS2, AtSMT2 and *AtCYP710A1* genes in Arabidopsis. The heat map generated by this program shows transcript expression of these genes under various elicitor-Arabidopsis interactions.

B, A diagram of T-DNA insertions to the gene CYP710A1. The mutant GK-325E09 has T-DNA inserted in the coding region of CYP710A1, i.e., 98 bp downstream from the start codon. The mutants Salk014626 and Salk112491 have T-DNA inserted upstream of the gene CYP710A1, i.e., 481 bp and 782 bp upstream from the start codon, respectively. More details of the GABI Kat 325E09 line are available at http://www.gabi-kat.de/db/showseq.php?line=325E09.

C, RT-qPCR showing *AtCYP710A1* gene transcripts in Arabidopsis *Atcyp710A1* mutants inoculated with *Psp*. Pathogen inoculation was performed as described in Ishiga *et al*., (2011). RT-qPCR was performed for leaf samples collected from *Psp* treated plants. Expression ratio relative to Col-0 buffer control samples were calculated. Error bars represent standard error values.

D, Six-week-old plants grown under control conditions were photographed, and aerial parts of the plant were oven-dried to calculate dry weight.

E, The Arabidopsis *Atcyp710A1* mutant compromises disease resistance. Plants were inoculated with *Psm* at a concentration of ~1×10^6 cfu/ml. Photographs were taken at 3 dpi.

Reference: Ishiga Y., Ishiga T., Uppalapati S. & Mysore K. (2011) Arabidopsis seedling flood-inoculation technique: A rapid and reliable assay for studying plant-bacterial interactions. *Plant Methods*, **7**, 32.

Supplemental Figure S6

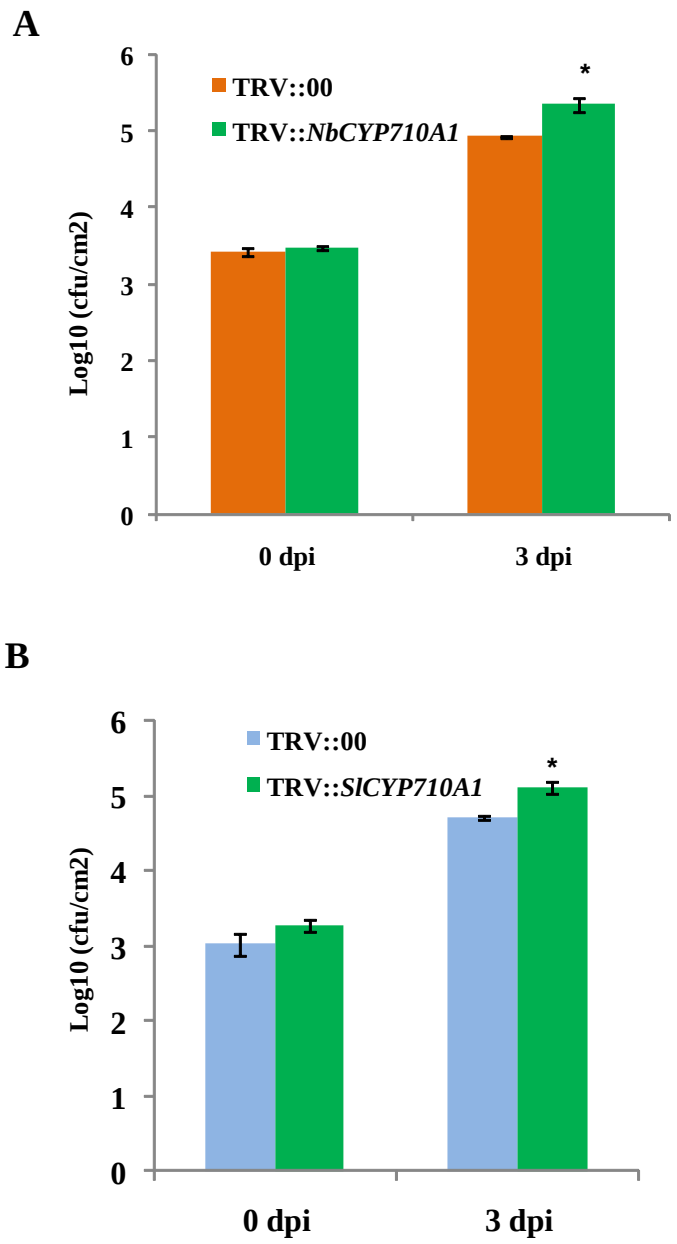

Supplemental Figure S6. Silencing of the *AtCYP710A1* gene by VIGS supports more multiplication of nonhost bacteria in *N. benthamiana* and tomato. A, Wild-type *N. benthamiana* plants were inoculated with TRV2::*NbCYP710A1*. Plants showing downregulation of this gene were inoculated with the nonhost pathogen *Pst* T1, and bacterial growth was assessed.
B, Wild-type tomato plants were inoculated with TRV2::*SlCYP710A1*. Plants showing downregulation of this gene were inoculated with the nonhost pathogen *Pstab*, and bacterial growth was assessed.
Error bars represent the standard error of mean values. * Significant difference at $p = 0.05$.

Supplemental Figure S7

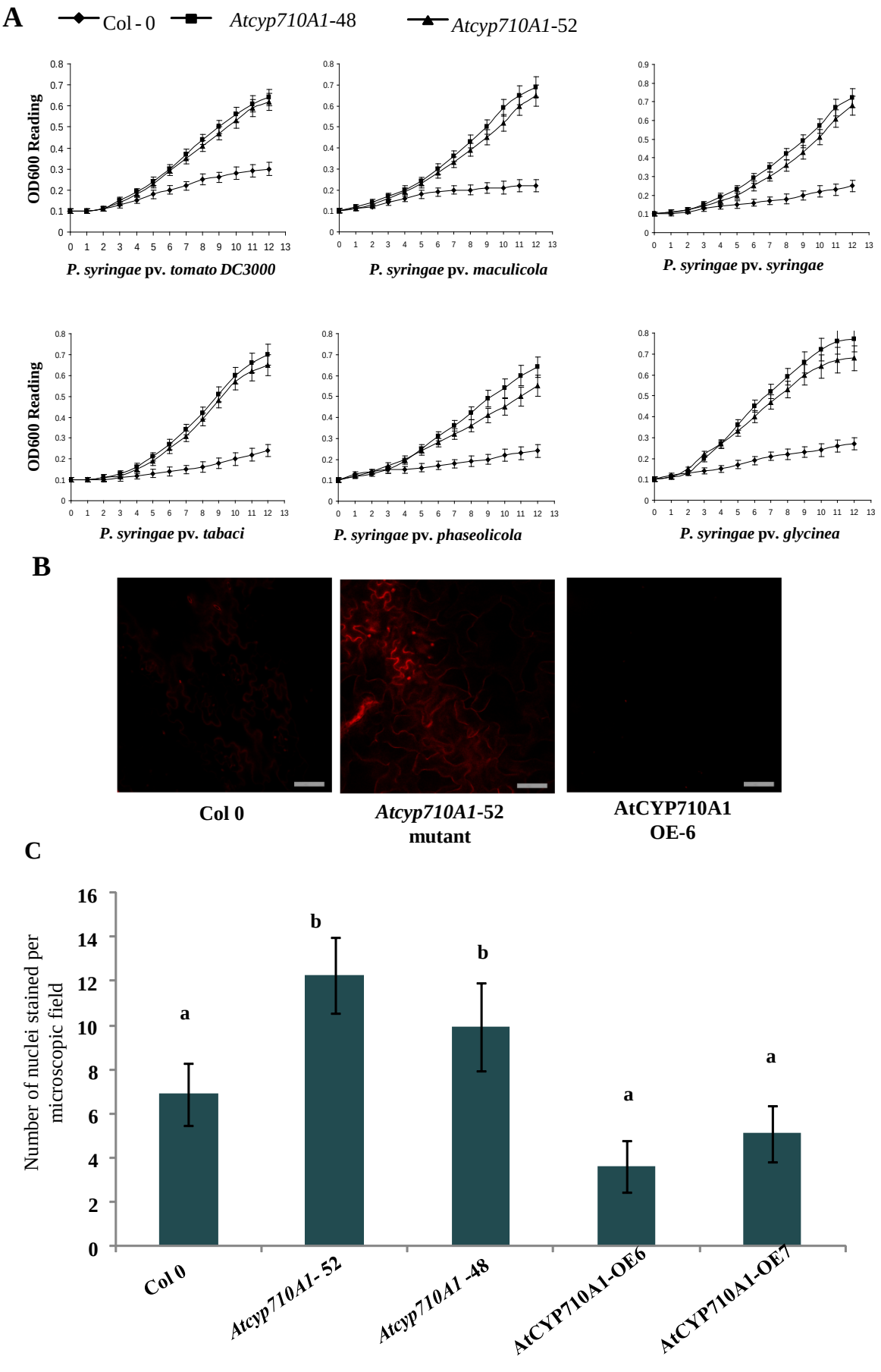

D

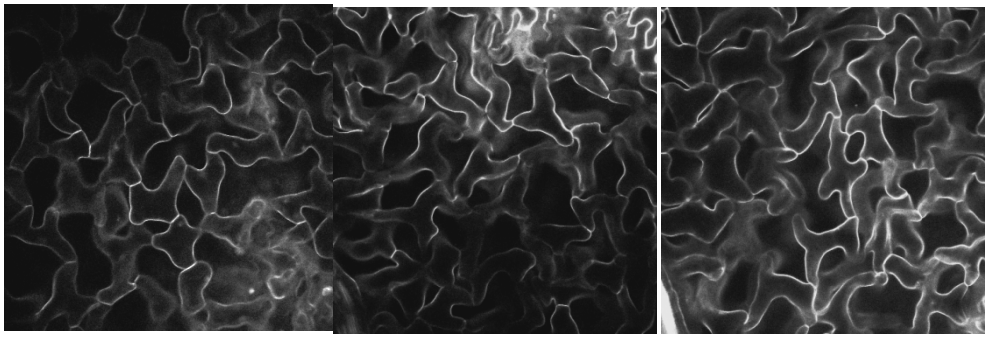

Col 0 | ***Atcyp710A1*-52 mutant** | **AtCYP710A1 OE-6**

Supplemental Figure S7. Analysis of pathogen growth in apoplastic fluid and membrane permeability characteristics. A, Bacterial growth in minimal medium containing 5% of apoplastic fluid. The leaves of Arabidopsis Col-0 and *Atcyp710A1* mutants (lines 48 and 52) were used to extract apoplastic fluid by the vacuum-centrifuge method. The filter-sterilized apoplastic fluid was added to minimal growth medium (MGM) to make 5% apoplastic fluid. Bacterial cells were collected by centrifugation of overnight culture, washed twice, resuspended in MGM and used to inoculate the fresh MGM with or without apoplastic fluid. Bacterial growth was determined by measuring the optical density at 600 nm (OD_{600}) of the bacterial culture every hour for 12 hours. Rectangles: MGM containing 5% of the apoplast extracted from Arabidopsis Col-0; Triangles: MGM containing 5% of the apoplast extracted from Arabidopsis *Atcyp710A1*-48; Round: MGM containing 5% of the apoplast extracted from Arabidopsis mutant *Atcyp710A1*-52. Error bars represent standard deviation values.
B and C, Assessing the penetration of propidium iodide dye. Leaf tissues were collected from Col 0, *Atcyp710A1* mutants and *AtCYP710A1* gene overexpressing plants, and incubated in propidium iodide solution. Sections were made from these leaf segments and observed for cells stained for their nuclei, and the number of cells showing nuclei staining were counted under confocal microscope. Error bars represent standard deviation values. Single factor ANOVA was performed ($p = 0.05$), and letters above each bar indicate the significance; same letter means values are not significantly different from each other.
D, To indicate the cell shape and size, pictures (grayscale) of the stained plasma membrane of cells from Col 0, *Atcyp710A1* mutants and *AtCYP710A1* plants were taken under the same field used in B. Sample preparation and imaging protocol is the same as explained in B.

Supplemental Figure S8

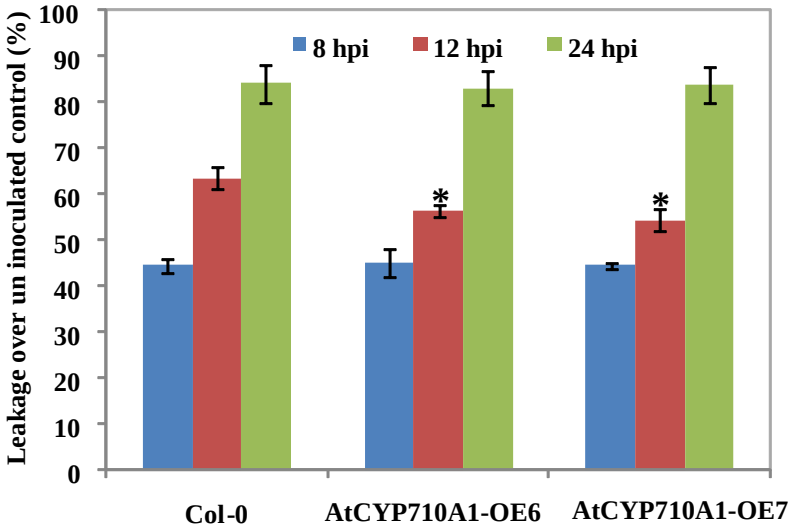

Supplemental Figure S8. Membrane leakage in *AtCYP710A1* overexpression plants upon host pathogen infection. Four-week-old *AtCYP710A1* overexpression plants were inoculated with the host pathogen *Psm*, and membrane leakage was assessed at different time points. * Significant difference at $p = 0.05$. Error bars represent standard error of mean values.